Metabolism Open 9 (2021) 100086

Contents lists available at ScienceDirect

Metabolism Open

journal homepage: www.journals.elsevier.com/metabolism-open

# The presence of 3-hydroxypropionate and 1,3-propanediol suggests an alternative path for conversion of glycerol to Acetyl-CoA

Eunsook S. Jin [a, b, *], Min H. Lee [a], Craig R. Malloy [a, b, c, d]

[a] Advanced Imaging Research Center, University of Texas Southwestern Medical Center, Dallas, TX, 75390, USA
[b] Department of Internal Medicine, University of Texas Southwestern Medical Center, USA
[c] Department of Radiology, University of Texas Southwestern Medical Center, USA
[d] VA North Texas Health Care System, Dallas, TX, 75216, USA

ARTICLE INFO

*Article history:*
Received 19 January 2021
Received in revised form
19 February 2021
Accepted 19 February 2021
Available online 26 February 2021

*Keywords:*
1,3-Propanediol
3-Hydroxypropionate
Gluconeogenesis
Oxidative metabolism
Aldehyde dehydrogenase
Ketogenesis

ABSTRACT

*Background:* In our recent study using [U−$^{13}C_3$]glycerol, a small subset of hamsters showed an unusual profile of glycerol metabolism: negligible gluconeogenesis from glycerol plus conversion of glycerol to 1,3-propanediol (1,3PDO) and 3-hydroxypropionate (3HP) which were detected in the liver and blood. The purpose of the current study is to evaluate the association of these unusual glycerol products with other biochemical processes in the liver.

*Methods:* Fasted hamsters received acetaminophen (400 mg/kg; n = 16) or saline (n = 10) intraperitoneally. After waiting 2 h, all the animals received [U−$^{13}C_3$]glycerol intraperitoneally. Liver and blood were harvested 1 h after the glycerol injection for NMR analysis and gene expression assays.

*Results:* 1,3PDO and 3HP derived from [U−$^{13}C_3$]glycerol were detected in the liver and plasma of eight hamsters (two controls and six hamsters with acetaminophen treatment). Glycerol metabolism in the liver of these animals differed substantially from conventional metabolic pathways. [U−$^{13}C_3$]glycerol was metabolized to acetyl-CoA as evidenced with downstream products detected in glutamate and β-hydroxybutyrate, yet $^{13}C$ labeling in pyruvate and glucose was minimal ($p < 0.001$, $^{13}C$ labeling difference in each metabolite). Expression of aldehyde dehydrogenases was enhanced in hamster livers with 1,3PDO and 3HP ($p < 0.05$).

*Conclusion:* Detection of 1,3PDO and 3HP in the hamster liver was associated with unorthodox metabolism of glycerol characterized by conversion of 3HP to acetyl-CoA followed by ketogenesis and oxidative metabolism through the TCA cycle. Additional mechanistic studies are needed to determine the causes of unusual glycerol metabolism in a subset of these hamsters.



## 1. Introduction

The pathways of glycerol metabolism in mammals are well-known. When the body uses triglycerides as an energy source, glycerol and fatty acids are released into the circulation. The concentration of circulating glycerol is generally less than 0.5 mM [1–3], but it may rise several fold during starvation, exercise and diabetes [3–5]. Glycerol in the bloodstream is predominantly utilized by the liver after phosphorylation via glycerol kinase, and it participates in gluconeogenesis, the glycolytic pathway, or fatty acid esterification. Glycerol metabolism in bacteria is also well-investigated and quite different from mammals. Glycerol is converted to glyceraldehyde via glycerol dehydrogenase (GlyDH) linked to $NAD^+$ [6,7] or to 3-hydroxypropionaldehyde (3HPA) via GlyDH in the presence of coenzyme $B_{12}$ [8–10]. The latter process occurs in some gut bacteria such as Lactobacillus reuteri and Klebsiella pneumonia. 3HPA is further metabolized [8–12]; the reduction of 3HPA via 1,3-propanediol oxidoreductase yields 1,3-propanediol (1,3PDO) while the oxidation of 3HPA via aldehyde dehydrogenase (ALDH) produces 3-hyroxypropionate (3HP).

*Abbreviations:* ACC, acetyl-CoA carboxylase; ALDH, aldehyde dehydrogenase; DHAP, dihydroxyacetone phosphate; G3P, glycerol 3-phosphate; GA3P, glyceraldehyde 3-phosphate; GAPDH, glyceraldehyde 3-phosphate dehydrogenase; GK, glycerol kinase; Glu, glutamate; GlyDH, glycerol dehydrogenase; β-HB, β-hydroxybutyrate; 3HP, 3-hydroxypropionate; 3HPA, 3-hydroxypropionaldehyde; α-kG, α-ketoglutarate; OAA, oxaloacetate; PCC, propionyl-CoA carboxylase; PDH, pyruvate dehydrogenase; 1,3PDO, 1,3-propanediol.

* Corresponding author. Advanced Imaging Research Center, 5323, Harry Hines Blvd., Dallas, TX, USA.
*E-mail address:* Eunsook.Jin@utsouthwestern.edu (E.S. Jin).

https://doi.org/10.1016/j.metop.2021.100086

1,3PDO is readily produced by the bacteria while 3HP production by natural microbiome was reported limited [9]. Production of 1,3PDO and 3HP using engineered bacterial strains has been extensively investigated because of multiple commercial applications [8,13–16]. However, these metabolites have received much less attention in association with host metabolism. It is also known that 3HP may rise in blood and urine of humans in the deficiency of propionyl-CoA carboxylase (PCC), a rare autosomal recessive disorder, causing propionic acidemia [17,18].

In an earlier study, we examined the impacts of glutathione depletion on the pentose phosphate pathway in the liver using analysis of $^{13}C$ distribution in plasma glucose after the administration of [U−$^{13}C_3$]glycerol [19]. The study group received a toxic dose of acetaminophen to deplete glutathione in the liver while controls received saline. Since all the animals (n = 16 with acetaminophen and n = 10 with saline) were overnight fasted prior to the administration of [U−$^{13}C_3$]glycerol, plasma glucose was highly enriched with $^{13}C$ in most hamsters, indicating active gluconeogenesis from glycerol, as anticipated. However, $^{13}C$-labeled glucose was nearly undetectable in eight hamsters (six acetaminophen-treated animals and two controls) due to minimal gluconeogenesis from the glycerol. Data from these hamsters were not reported previously [19], and they were re-examined. Unexpectedly, we found detectable.1,3PDO and 3HP in the liver and the blood of these animals and co-existing substantial changes in hepatic metabolism in the presence of the glycerol products.

The aims of this study are to report unusual glycerol metabolism in the liver in the presence of 1,3PDO and 3HP and to suggest the underlying pathway of glycerol metabolism to acetyl-CoA after the generation of these products. The appearance of 1,3PDO and 3HP in the liver of mammals is surprising because they are typically known as metabolites derived from the gut microbiome. To our knowledge this is the first report of unexpected hepatic metabolism in association with these unusual products of glycerol. After the administration of [U−$^{13}C_3$]glycerol, this subset of hamsters was characterized by negligible gluconeogenesis and increased ketogenesis. The production of 1,3PDO and 3HP from glycerol was also associated with oxidative metabolism of glycerol through the TCA cycle.

## 2. Methods

### 2.1. Animal studies

The study was approved by the Institutional Animal Care and Use Committee at the University of Texas Southwestern Medical Center. Male golden Syrian hamsters were purchased from Charles Rivers Laboratories (Wilmington, MA). All animals were placed on a 12:12-h day-night cycle and had free access to rodent chow and water. Chow was withdrawn at 4 p.m. for an overnight fast. At 9 a.m. on the next day, a group of hamsters (n = 16; 141 ± 3 g) received acetaminophen (400 mg/kg) dissolved in warm saline (2 mL) intraperitoneally under isoflurane® anesthesia while the other group of hamsters (n = 10; 144 ± 4 g) received saline only. Hamsters quickly awakened and remained physically active. After waiting 2 h, all hamsters received [U−$^{13}C_3$]glycerol (50%, 100 mg/kg; Cambridge Isotopes, Andover, MA) dissolved in deionized water (1 mL) intraperitoneally in an abdominal site under anesthesia. Again, they awakened quickly and were physically active. After 1 h, they were sacrificed under general anesthesia. Blood was harvested from the inferior vena cava, and the liver was excised and freeze-clamped with aluminum tongs at liquid nitrogen temperature. Plasma and liver tissue were kept at −80 °C prior to further processing.

### 2.2. Sample processing for NMR acquisition

Liver tissue was ground in liquid nitrogen using a mortar and pestle. Ground tissue (3 g) was treated with cold perchloric acid (10%, 15 mL) to extract water-soluble metabolites. Plasma (4–6 mL) was also treated using perchloric acid (70%) to a final concentration of 10%. The mixture was vortexed for 1 min, centrifuged and the supernatant was transferred to a new tube. After repeating the extraction, the supernatant was adjusted to pH 8 using KOH solutions. The mixture was centrifuged and the supernatant was transferred and lyophilized.

### 2.3. NMR acquisition

$^{13}C$ NMR spectra were collected using a 14.1T spectrometer (Varian INOVA, Agilent, Santa Clara, CA) equipped with a 3-mm broadband probe with the observe coil tuned to $^{13}C$ (150 MHz). The samples were dissolved in $^{2}H_2O$ (300 μL for liver extracts and 200 μL for plasma extracts) containing 4,4-dimethyl-4-silapentane-1-sulfonic acid (DSS; 5 mM), centrifuged, and the supernatant was transferred to a 3-mm NMR tube. NMR spectra of the extracts or reference chemicals, 1,3PDO and 3HP (Sigma, St. Louis, MO), were acquired using a 45° pulse, a 36,765-Hz sweep width, 55,147 data points and a 1.5-s acquisition time with 1.5-s interpulse delay at 25 °C. Proton decoupling was performed using a standard WALTZ-16 pulse sequence. Spectra averaged approximately 23,000 scans requiring 20 h. All NMR spectra were analyzed using ACD/Labs NMR spectral analysis program (Advanced Chemistry Development, Inc., Toronto, Canada).

### 2.4. $^{13}C$ NMR analysis for metabolite quantitation and $^{13}C$ enrichment

The relative concentration of each metabolite was calculated using a singlet from the metabolite normalized by the signal of DSS. The singlet from natural $^{13}C$ abundance reflects the pool size of a metabolite. Excess $^{13}C$ enrichment in metabolites was calculated using a doublet, the signal due to $^{13}C$–$^{13}C$ spin-spin coupling, based on an assumption that a singlet was natural abundance (1.1%). In addition, the relative levels of $^{13}C$-labeled metabolites in $^{13}C$ NMR spectra were calculated using the peak areas of specified doublets normalized by the peak area of DSS. Glucose concentration in plasma was measured using glucose oxidase method (YSI 2300 Glucose Analyzer; GMI, Inc).

### 2.5. RNA extraction and real-time quantitative PCR analysis

Total RNA was isolated from the liver of hamsters using TRIzol (Ambion, Carlsbad, CA). Complementary DNA (cDNA) was synthesized from 1 μg total RNA with oligo-dT primers using high capacity cDNA reverse transcription kit according to the manufacturer's protocol (Applied Biosystems, Grand Island, NY) on the S1000™ Thermal cycler (Bio rad laboratories, Hercules, CA). Real-time quantitative PCR (RT–qPCR) was performed with the iTaq™ Universal SYBR® Green Supermix (Bio rad laboratories, Hercules, CA) on the CFX384™ real time system (Bio rad laboratories). The results were normalized by a housekeeping gene, glyceraldehyde 3-phosphate dehydrogenase (GAPDH). The followings are PCR primers for acetyl-CoA carboxylase (ACC), aldehyde dehydrogenase (ALDH), PCC and GAPDH.

| Gene | Primer Sequence |
|---|---|
| ACACA | 5′-CTTGGAGCAGAGAACCTTCG-3′; 5′-CAAGGTAAGCCCCAATACCA-3′ |
| ACACB | 5′-ATGTCACCAAGGACCTGCTC-3′; 5′-AAAGAGAGCCTGCCTGAACA-3′ |
| ALDH1A3 | 5′-GGCCATTACACCATGGAACT-3′; 5′-ACCCGACCTCTTTGATGAGA-3′ |
| ALDH2 | 5′-TCCTACCTGGTGGATTTGGA-3′; 5′-GCGGGTGTAGCTGAAGAAGT-3′ |
| ALDH3A2 | 5′-ATTCTTTGCCCTTTGGAGGT-3′; 5′-CTGTTGGGAGGGTACCTGAG-3′ |
| ALDH7A1 | 5′-AGACTGTGGCATTGTGAACG-3′; 5′-CGCATGTACTGCTTCCAGG-3′ |
| GAPDH | 5′-AACTTTGGCATTGTGGAAGG-3′; 5′-GGATGCAGGGATGATGTTCT-3′ |
| PCCA | 5′-ATGTCGGGTTTATGCTGAGG-3′; 5′-TTGGATGCCACTGTCAACTC-3′ |

### 2.6. Statistics

Data are expressed as mean ± SEM. Comparisons between two groups were made using a student's t-test, where $p < 0.05$ was considered significant.

## 3. Results

### 3.1. $^{13}C$ NMR detection of 1,3PDO and 3HP in the liver and plasma

Two unexpected metabolites, 1,3PDO and 3HP derived from [U−$^{13}C_3$]glycerol, were detected in extracts from the liver and plasma of eight hamsters (Fig. 1A). Six of these animals had received acetaminophen and the remaining two hamsters had not. $^{13}C$ NMR spectra of the extracts from these animals showed characteristic multiplet signals from [U−$^{13}C_3$]1,3PDO and [U−$^{13}C_3$]3HP. The multiplets (D, doublet; T, triplet; Q, quartet) arose due to $^{13}C$−$^{13}C$ spin-spin couplings in 1,3PDO ($J_{12} = J_{23} = 37$ Hz coupling constant) and 3HP ($J_{12} = 51$ Hz; $J_{23} = 37$ Hz). The chemical shifts and coupling constants of these metabolites were confirmed using standard chemicals with natural $^{13}C$ abundance.

Glycerol metabolism differed dramatically in the liver of these animals with 1,3PDO and 3HP. The changes in hepatic metabolism were essentially the same regardless of acetaminophen treatment, but the data from two control hamsters with 1,3PDO and 3HP were not included in statistical data in the current study. Statistical analysis was performed using the data from acetaminophen-treated hamsters only; the absence of 1,3PDO and 3HP ($n = 10$) versus the presence of 1,3PDO and 3HP ($n = 6$).

The content of [U−$^{13}C_3$]1,3PDO in the liver was determined by measuring the area of the doublet from 1,3PDO C1&C3 normalized by DSS (Fig. 1B). The same procedure was used to measure the content of [U−$^{13}C_3$]3HP in the liver by referencing the doublet of 3HP at the C3 relative to DSS. The content of 3HP in the liver was higher than that of 1,3PDO. Statistical correlation cannot be determined due to a small sample size, but the level of 3HP paralleled the level of 1,3PDO in the liver (Fig. 1C). The signals from [U−$^{13}C_3$] 1,3PDO and [U−$^{13}C_3$]3HP were presented together with those from [U−$^{13}C_3$]glycerol and [U−$^{13}C_3$]glycerol 3-phopshate (G3P) for comparison (Fig. 1D). In the absence of 1,3PDO and 3HP, animals had strong doublet signals from [U−$^{13}C_3$]glycerol and [U−$^{13}C_3$]G3P in the liver, and from [U−$^{13}C_3$]glycerol in plasma. In the presence of 1,3PDO and 3HP, however, doublet signals from these $^{13}C$-labeled glycerol and G3P were minimal (Fig. 1D).

### 3.2. Minimal glycerol phosphorylation and gluconeogenesis in the liver with 1,3PDO and 3HP

In the normal liver, glycerol phosphorylation produces glycerol 3-phosphate (G3P) that may be converted to other trioses such as dihydroxyacetone phosphate (DHAP) and glyceraldehyde 3-phosphate (GA3P). GA3P is metabolized to pyruvate through the glycolytic pathway while condensation of GA3P and DHAP leads to glucose through gluconeogenesis. In $^{13}C$ NMR of liver extracts, glycerol and G3P with natural $^{13}C$ abundance (S, singlet, in Fig. 2A) were detected in all animals regardless of detecting 1,3PDO and 3HP. However, signals from [U−$^{13}C_3$]glycerol and [U−$^{13}C_3$]G3P (D, doublet, in Fig. 2A) were minimal in the liver from animals with 1,3PDO and 3HP. Conversely, signals from [U−$^{13}C_3$]glycerol and [U−$^{13}C_3$]G3P were readily identified in animals without the glycerol products. The concentrations of glycerol and G3P were unchanged in the livers with 1,3PDO and 3HP, but their $^{13}C$ enrichments were dramatically reduced (Fig. 2B). Since doublet signal from [U−$^{13}C_3$]glycerol was also minimal in hamster plasma with 1,3PDO and 3HP, the difference in $^{13}C$ enrichments was due to reduced delivery of [U−$^{13}C_3$]glycerol to the liver.

After the administration of [U−$^{13}C_3$]glycerol, triple-labeled ([1,2,3−$^{13}C_3$] and [4,5,6−$^{13}C_3$]) glucose appears as a consequence of direct gluconeogenesis (Fig. 2C). [1,2,3−$^{13}C_3$]glucose produces a doublet in glucose C1 region due to $^{13}C$−$^{13}C$ scalar coupling, $J_{12}$, whereas natural abundant glucose is detected as a singlet. In the $^{13}C$ NMR of liver extracts, the doublet signal from [1,2,3−$^{13}C_3$]glucose was strong in animals without 1,3PDO and 3HP. However, among animals with detectable.1,3PDO and 3HP, the glucose C1 doublet was minimal, indicating little conversion of [U−$^{13}C_3$]glycerol to glucose. The concentration of glucose in the liver and plasma were unchanged in the presence of 1,3PDO and 3HP (Fig. 2D), indicating preservation of overall glucose homeostasis. These data also indicate that delivery of [U−$^{13}C_3$]glycerol to the liver for gluconeogenesis was substantially reduced in these animals.

### 3.3. Active ketogenesis and oxidative metabolism through the TCA cycle in the liver with 1,3PDO and 3HP

Pyruvate is in rapid exchange with lactate and alanine in the cytosol and $^{13}C$ enrichment in pyruvate is reflected by the enrichments in lactate and alanine. After entering the mitochondrion, pyruvate is decarboxylated via pyruvate dehydrogenase, producing acetyl-CoA (Fig. 3A). Acetyl-CoA is further metabolized to acetate, ketone bodies including β-hydroxybutyrate, or citrate in the TCA cycle. In $^{13}C$ NMR of liver extracts, signals from [U−$^{13}C_3$]lactate and [U−$^{13}C_3$]alanine are readily detected in the liver without 1,3PDO and 3HP, but they were substantially reduced in the liver with 1,3PDO and 3HP. Paradoxically, signals from [U−$^{13}C_2$]acetate, [1,2−$^{13}C_2$]- and [3,4−$^{13}C_2$]β-hydroxybutyrate, and [4,5−$^{13}C_2$]glutamate were enhanced in the liver with 1,3PDO and 3HP (Fig. 3B). The condensation of [1,2−$^{13}C_2$]acetyl-CoA and oxaloacetate produces [4,5−$^{13}C_2$]citrate and consequently [4,5−$^{13}C_2$]α-ketoglutarate through the TCA cycle (Fig. 3A). Since α-ketoglutarate is in exchange with glutamate, the appearance of [4,5−$^{13}C_2$]glutamate indicates oxidative metabolism of [U−$^{13}C_2$]acetyl-CoA through the TCA cycle. These findings in acetate, β-hydroxybutyrate and glutamate were surprising because $^{13}C$ labeling in lactate and alanine indicated low enrichment in upstream pyruvate.

The concentrations of lactate and alanine were unchanged in the liver with 1,3PDO and 3HP, but $^{13}C$ enrichments in these

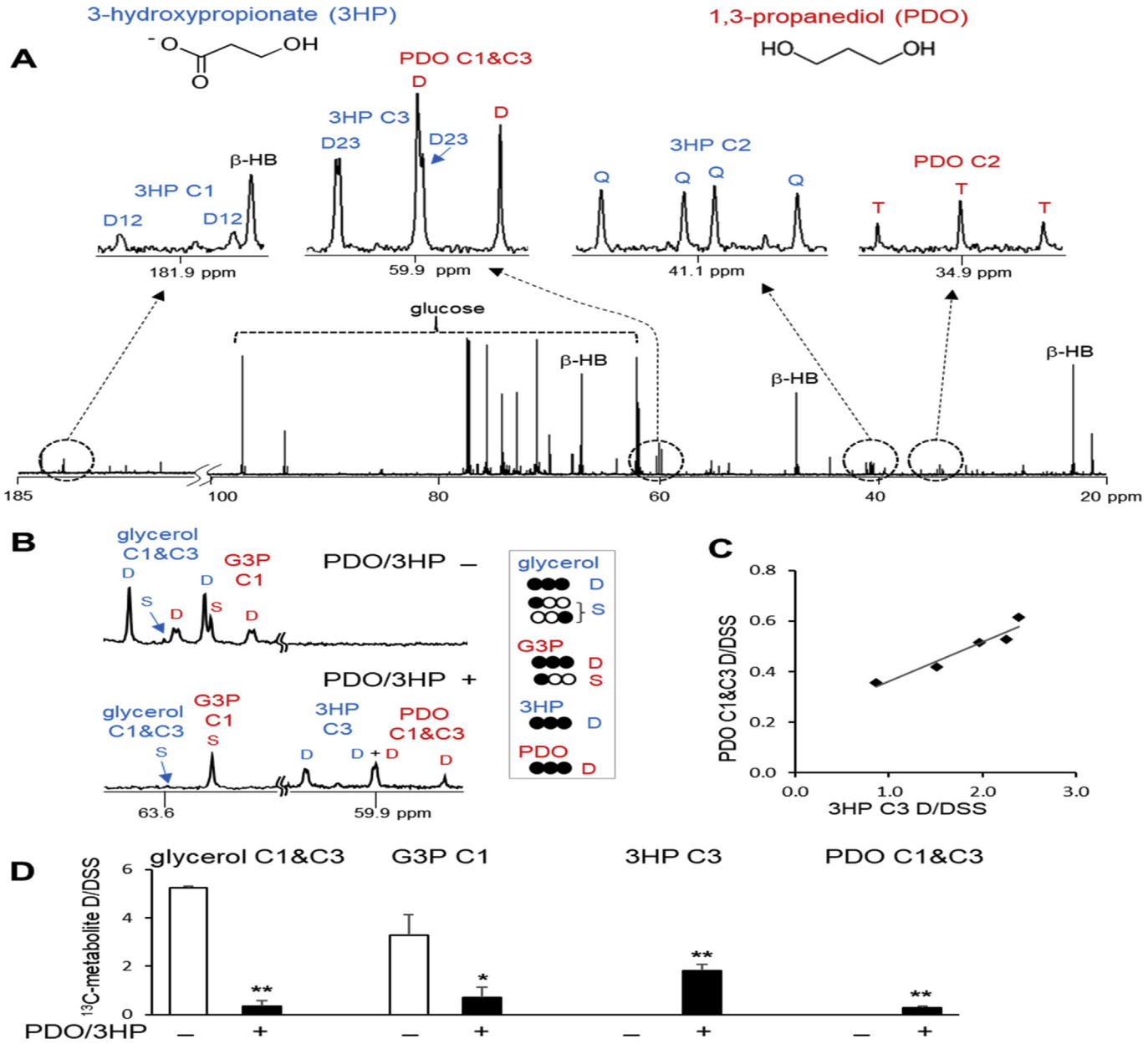


**Fig. 1. 1,3-propanediol and 3-hydroxypropionate detection.** (**A**) $^{13}C$ NMR of plasma extracts from a hamster receiving [U−$^{13}C_3$]glycerol shows multiplets from [U−$^{13}C_3$]1,3-propanediol (PDO) and [U−$^{13}C_3$]3-hydroxypropionate (3HP). The chemical shifts of 1,3PDO are 34.9 ppm (C2) and 59.8 ppm (C1 & C3), and those of 3HP are 41.1 ppm (C2), 60.0 ppm (C3) and 181.9 ppm (C1). Multiplets (D, doublet; T, triplet; Q, quartet) are due to $^{13}C$–$^{13}C$ spin-spin couplings in these metabolites. (**B**) $^{13}C$ NMR spectra of liver extracts show resonance at glycerol C1&C3 (63.6 ppm), G3P C1 (63.5 ppm), 3HP C3 (60.0 ppm) and 1,3PDO C1&C3 (59.8 ppm). In the absence of 1,3PDO and 3HP, doublet signals from $^{13}C$-labeled glycerol and G3P are well detected along with singlets with natural abundance. In the presence of 1,3PDO and 3HP, however, doublet signals from [U−$^{13}C_3$]glycerol and [U−$^{13}C_3$]G3P are minimal while singlets are still detectable. (**C**) A graph shows that the content of [U−$^{13}C_3$]3HP parallels that of [U−$^{13}C_3$]1,3PDO based on doublet signals in $^{13}C$ NMR of liver extracts. (**D**) In the analysis of $^{13}C$ NMR of liver extracts, doublet signals from $^{13}C$-labeled glycerol, G3P, 3HP and 1,3PDO were normalized by DSS (NMR reference). [U−$^{13}C_3$] glycerol and [U−$^{13}C_3$]G3P were minimal in the presence of [U−$^{13}C_3$]3HP and [U−$^{13}C_3$]1,3PDO. Abbreviations: D, doublet; D12, doublet from coupling of C1 with C2; D23, doublet from coupling of C2 with C3; Q, quartet arising from coupling of C2 with both C1 and C3; β-HB, β-hydroxybutyrate; S, singlet; T, triplet arising from coupling of C2 with both C1 and C3; *, $p < 0.05$; **, $p < 0.001$; $n = 5–8$ in each group.

metabolites were substantially reduced (Fig. 3C and D). The concentration of β-hydroxybutyrate and its $^{13}C$ enrichment were increased in the hamster liver with 1,3PDO and 3HP (Fig. 3E). The level of acetate was unchanged, but its $^{13}C$ enrichment was increased in the liver with 1,3PDO and 3HP (Fig. 3F). Metabolism through the TCA cycle was also activated in the liver with 1,3PDO and 3HP because the concentration of glutamate was increased and [4,5−$^{13}C_2$]glutamate was detected only in the liver with 1,3PDO and 3HP (Fig. 3G).

### *3.4. Enhanced aldehyde dehydrogenase expression in the liver with 1,3PDO and 3HP*

Genes involved in 3HP production in the liver were examined including ACC, PCC and ALDH. ACC catalyzes the irreversible carboxylation of acetyl-CoA to produce malonyl-CoA that is converted to 3HP through malonate semialdehyde. PCC catalyzes the carboxylation of propionyl-CoA to methylmalonyl-CoA, and the deficiency of PCC, as seen in propionic acidemia, leads to 3HP and

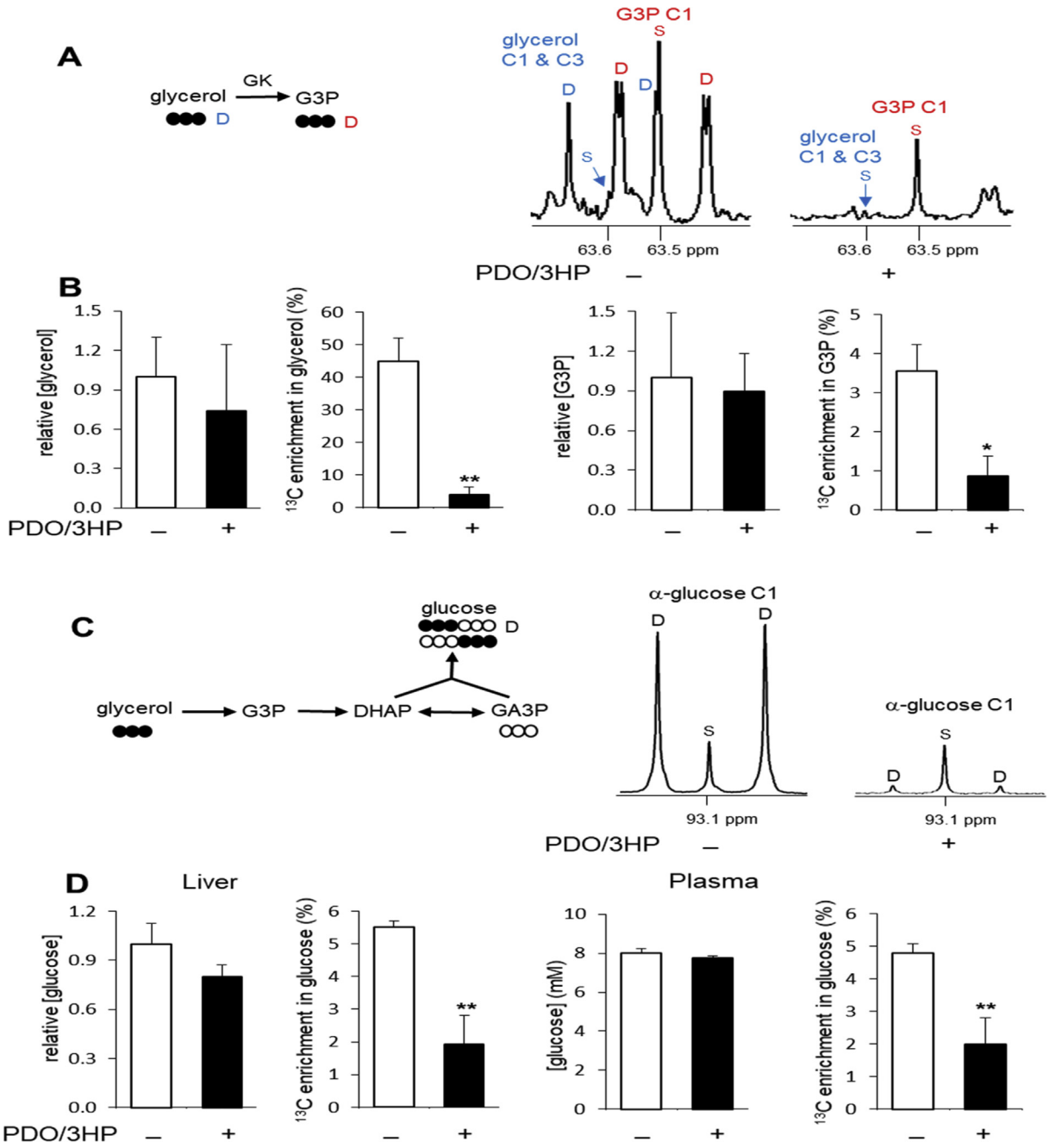


**Fig. 2. Minimal glycerol phosphorylation and gluconeogenesis in the liver with 1,3PDO and 3HP.** (**A**) In $^{13}C$ NMR of glycerol C1&C3 and glycerol 3-phosphate (G3P) C1 from liver extracts, singlet (S) signals are from natural $^{13}C$ abundance and they are detected in all hamsters. However, doublet (D) signals from [U−$^{13}C_3$]glycerol and [U−$^{13}C_3$]G3P are negligible in the liver with 1,3PDO and 3HP while they are strong in the liver without 1,3PDO and 3HP. (**B**) The concentrations of glycerol and G3P were unaltered, but their $^{13}C$ enrichments were decreased in the liver with 1,3PDO and 3HP. (**C**) In $^{13}C$ NMR of α-glucose C1, a singlet (S) reflects [1−$^{13}C_1$]glucose with natural abundance while a doublet (D) is from [1,2,3−$^{13}C_3$]glucose. The doublet reflects gluconeogenesis from [U−$^{13}C_3$]glycerol. (**D**) The concentrations of glucose in the liver and plasma were unchanged, but their $^{13}C$ enrichments were reduced in the presence of 1,3PDO and 3HP. Abbreviations: DHAP, dihydroxyacetone phosphate, GA3P, glyceraldehyde 3-phosphate; open circle, $^{12}C$; black circle, $^{13}C$; *, $p < 0.05$; **, $p < 0.001$, $n = 6–10$ in each group.

propionic acid. ALDH catalyzes the oxidation of aldehyde and it produces 3HP from 3HPA (Fig. 4A). The mRNA expressions of ACC isoforms (ACACA and ACACB) and PCC (PCCA) were not altered in the liver with 1,3PDO and 3HP, but some of ALDH isoforms (ALDH3A2 and ALDH7A1) were increased (Fig. 4B).

## 4. Discussion

This study identified 1,3PDO and 3HP derived from glycerol in the liver and the circulation of a subset of hamsters, and detection of both products was associated with significant disruption of hepatic metabolism. The usual pathways of glycerol metabolism – phosphorylation followed by incorporation into gluconeogenesis or glycolysis - were minimal in the hamster livers with 1,3PDO and 3HP. Surprisingly, glycerol metabolism to β-hydroxybutyrate and glutamate was stimulated despite minimal glycerol conversion to pyruvate. This study demonstrated that glycerol metabolism to 1,3PDO and 3HP interrupted gluconeogenesis but activated

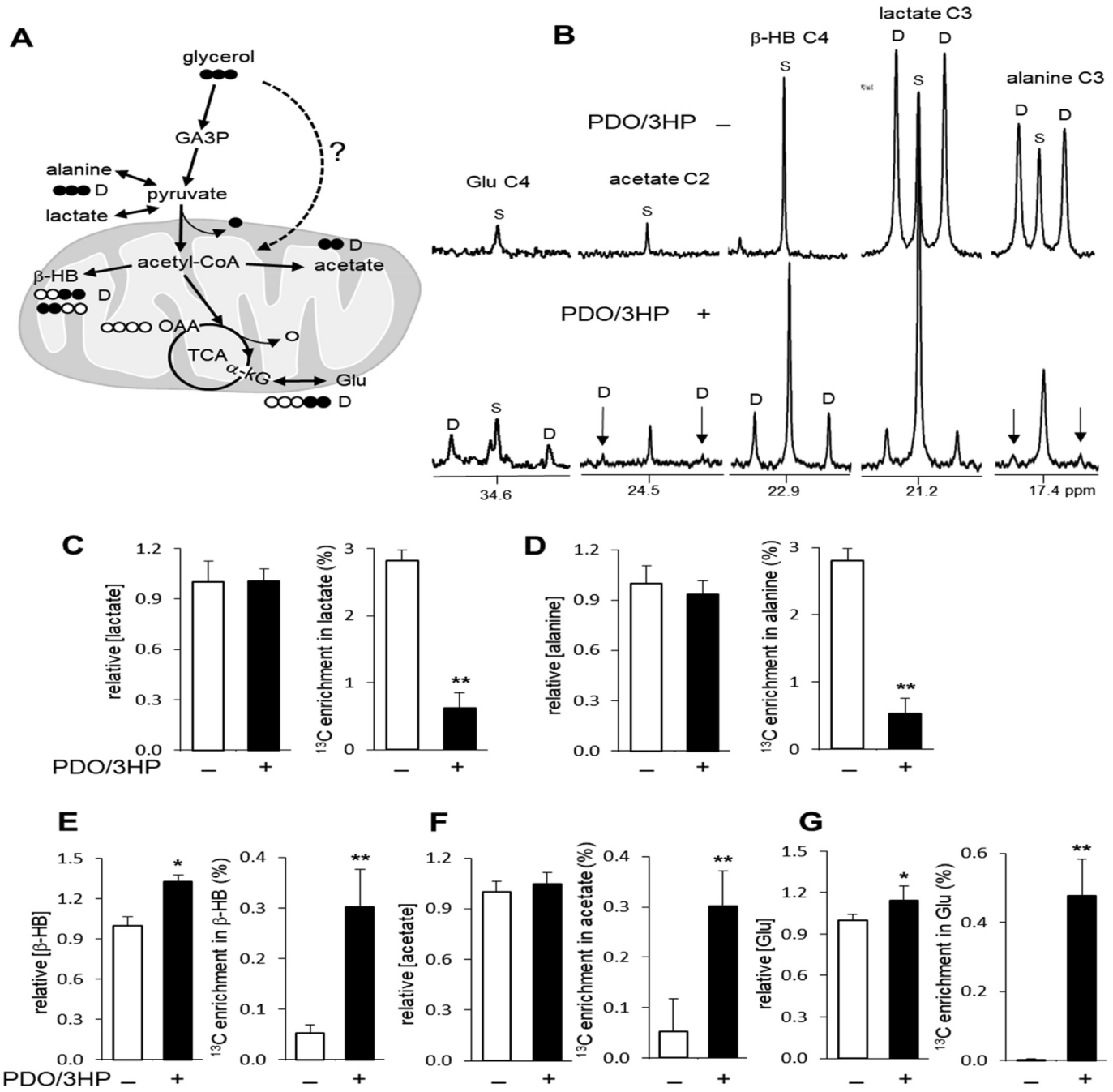


**Fig. 3. Ketogenesis and oxidative metabolism through the TCA cycle in the liver with 1,3PDO and 3HP.** (**A**) A schematic shows routes from glycerol to acetyl-CoA that is further metabolized to acetate, β-hydroxybutyrate (β-HB) or the TCA cycle. (**B**) In $^{13}C$ NMR of liver extracts, doublet (D) signals from [4,5−$^{13}C_2$]glutamate (Glu), [3,4−$^{13}C_2$]β-hydroxybutyrate and [1,2−$^{13}C_2$]acetate are stronger while the signals from [U−$^{13}C_3$]lactate and [U−$^{13}C_3$]alanine are substantially lower in the liver with 1,3PDO and 3HP compared to the liver without them. (**C-D**) The concentrations of lactate and alanine were unchanged, but their $^{13}C$ enrichments were reduced in the liver with 1,3PDO and 3HP. (**E**) The concentration of β-hydroxybutyrate and its $^{13}C$ enrichment were increased in the liver with 1,3PDO and 3HP. (**F**) Acetate concentration was unchanged, but its $^{13}C$ enrichment was increased in the liver with 1,3PDO and 3HP. (**G**) The concentration of glutamate and its enrichment by [4,5−$^{13}C_2$]glutamate were increased in the liver with 1,3PDO and 3HP. Abbreviations: α-kG, α-ketoglutarate; *, $p < 0.05$; **, $p < 0.001$; $n = 6–10$ in each group.

catabolism through unusual pathways in the liver.

Conventional metabolic pathways in the liver are not consistent with the $^{13}C$-labeling patterns of metabolites in the presence of 1,3PDO and 3HP. The well-established pathways from glycerol to lactate, alanine and acetyl-CoA occur through glycerol phosphorylation followed by the glycolytic pathway. Pyruvate produced through glycolysis is in exchange with lactate and alanine, or decarboxylated to acetyl-CoA. Glucose is also readily produced from glycerol through the condensation of GA3P and DHAP. These processes were expected and confirmed by strong signals from $^{13}C$-labeled glucose, lactate, alanine and G3P after the administration of [U−$^{13}C_3$]glycerol in the livers *without* 1,3PDO and 3HP. However, livers *with* 1,3PDO and 3HP had minimal $^{13}C$-labeling in these metabolites (Figs. 2 and 3). Interestingly, however, downstream products of acetyl-CoA had enhanced $^{13}C$-labeling based on the signals from [1,2−$^{13}C_2$]- and [3,4−$^{13}C_2$]β-hydroxybutyrate,

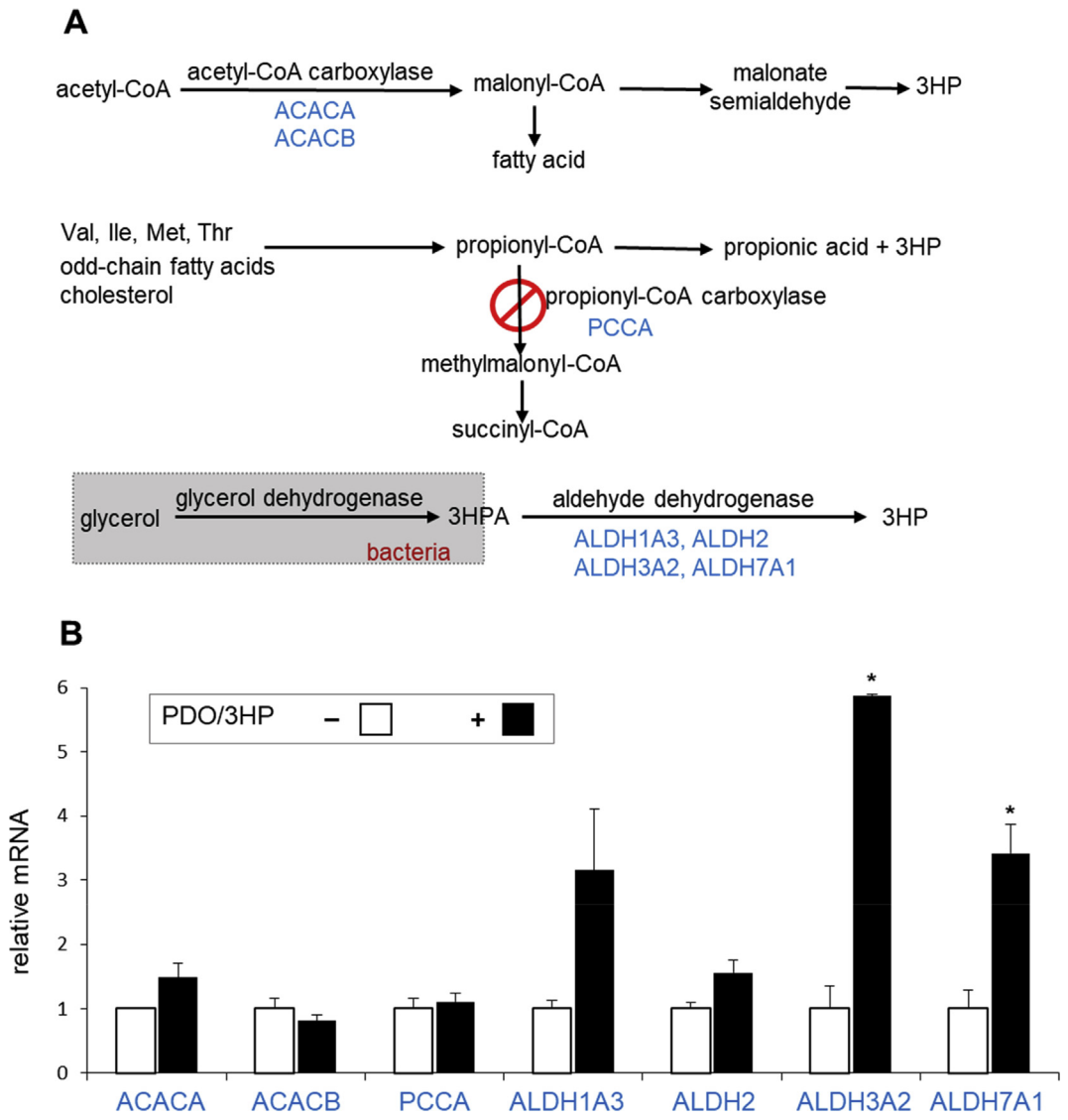


**Fig. 4. Enhanced aldehyde dehydrogenase expressions in the liver with 1,3PDO and 3HP**. (**A**) Schematics show metabolic processes involved in the production of 3HP. 3HP can be produced from acetyl-CoA through acetyl-CoA carboxylase (ACC). The lack of propionyl-CoA carboxylase (PCC) accumulates propionyl-CoA, which leads to 3HP and propionic acid production. Glycerol dehydrogenase converts glycerol to 3HPA that is further metabolized to 3HP via aldehyde dehydrogenase (ALDH). (**B**) A graph shows mRNA expressions of enzymes associated with 3HP production. Two isoforms of ALDH (ALDH3A2 and ALDH7A1) were increased in the liver with 1,3PDO and 3HP, but ACC and PCC remained unchanged. Abbreviations: 3HPA, 3-hydroxypropionaldehyde; *, $p < 0.05$; $n = 2$ in each group.

[1,2−$^{13}C_2$]acetate and [4,5−$^{13}C_2$]glutamate (Fig. 3). All these double-labeled metabolites indicated the presence of [1,2−$^{13}C_2$] acetyl-CoA. However, since $^{13}$C-labeling in upstream pyruvate was minimal in the liver with 1,3PDO and 3HP, the conversion of [U−$^{13}C_3$]glycerol to [1,2−$^{13}C_2$]acetyl-CoA is not consistent with the standard pathways of glycerol metabolism and must occur through unconventional pathways that bypass pyruvate.

Three alternative models were considered to understand the evidence for unusual glycerol metabolism observed in the current study. One hypothesis is that all these findings occurred through under-appreciated pathways in the mammalian liver. The liver can convert glycerol to 3HP through acetyl-CoA and malonyl-CoA [20,21] after entering the glycolytic pathway, as briefly illustrated in Fig. 4A. However, the liver metabolism alone cannot explain the production of 1,3PDO. The production of 3HP paralleled that of 1,3PDO (Fig. 1C), which strongly suggested a common pathway for the two products through 3HPA. However, glycerol conversion to 3HPA via GlyDH in mammals has not been reported to our knowledge. Another hypothesis is that the findings occurred via gut microbiome. As noted, some microbiome such as Lactobacillus reuteri and Klebsiella pneumonia converts glycerol to 1,3 PDO and 3HP through 3HPA [8–10]. However, this hypothesis is not fully consistent with the current data, either, because natural microbiome was reported to have minimal activities of ALDH enzymes to produce 3HP [9,22,23]. In addition, bacteria do not have mitochondria and they have an incomplete TCA cycle [24]. Thus, enhanced ketogenesis and oxidative metabolism through the TCA cycle in the presence of 1,3PDO and 3HP cannot be explained by microbial metabolism alone. The third hypothesis is that these findings required some interaction between the microbiome and the liver. Because ALDH expressions were enhanced in the hamster liver with 1,3PDO and 3HP, the combination of these findings and earlier studies of glycerol metabolism in microbiome suggests that 3HPA generated from glycerol by gut bacteria was presumably metabolized to 3HP via ALDH in the liver. It was also reported that liver converts 3HP to acetyl-CoA through malonate semialdehyde

[20,21]. Thus, it is more likely that $^{13}$C-labeled β-hydroxybutyrate and glutamate were downstream products of [1,2−$^{13}C_2$]acetyl-CoA in the liver derived from [U−$^{13}C_3$]3HP (Fig. 5).

The significance of 1,3PDO and 3HP production is not clear, nor is the relevance of these metabolites for the general health of the host despite the dramatic changes in liver metabolism. The hamsters with 1,3PDO and 3HP did not show any unusual external signs of distress. Healthy humans also have trace amounts of 1,3PDO and 3HP in plasma and urine [25]. 1,3PDO seems not to be toxic [26], but accumulated 3HP is associated with acidosis. 3HP is one of diagnostic metabolites in propionic acidemia caused by the deficiency of PCC [17,18]. There are few reports regarding these products in the association with host health, but an early study reported high concentrations of the products in the urine of patients who died in infancy [27]. Since glycerol was utilized for catabolism instead of gluconeogenesis in the presence of 1,3PDO and 3HP, this unusual glycerol metabolism may conceivably contribute to glycemic control. Glycerol is an important substrate for gluconeogenesis, and glucose production derived from this substrate may increase in type 2 diabetic patients [28]. Thus, glycerol oxidation through the TCA cycle instead of its conversion to glucose would ameliorate hyperglycemia. If we assume that these metabolites were produced via microbiome, however, the translocation of bacterial products to the liver meant leaky gut barrier. In addition, most animals with 1,3PDO and 3HP in the current study had minimal glutathione in the liver due to an acetaminophen overdose [19]. It is known that an aldehyde (-CHO) of 3HPA reacts with a thiol (-SH) of glutathione or proteins [22,29,30]. The shortage of glutathione in the liver might drive 3HPA conversion to 3HP instead of detoxification by glutathione.

The current study has limitations. First, the mechanism for production of these unusual products is not known. The results from measurements of ALDH expression may account for production of 3HP from 3HPA, but the direct causes of glycerol conversion to 3HP and 1,3PDO are unknown. Second, this study does not demonstrate microbial involvement, although the unanticipated products and labeling patterns are consistent with commonly known microbial processes. It remains to be investigated whether and what type of microbiome is associated with glycerol metabolism to 1,3PDO and 3HP. Third, it is unknown if there are any long-term effects of unusual glycerol metabolism for the general health of the host. Finally, it also remains to be investigated if the unexpected metabolism observed in a subset of hamsters occurs in human subjects.

In summary, a subset of hamsters receiving glycerol had detectable 1,3PDO and 3HP in the liver and the circulation, a finding that was associated with impaired gluconeogenesis from glycerol. These animals utilized glycerol for both ketogenesis and oxidative metabolism through acetyl-CoA. It remains to be investigated what triggered the appearance of 1,3PDO and 3HP in the liver of these

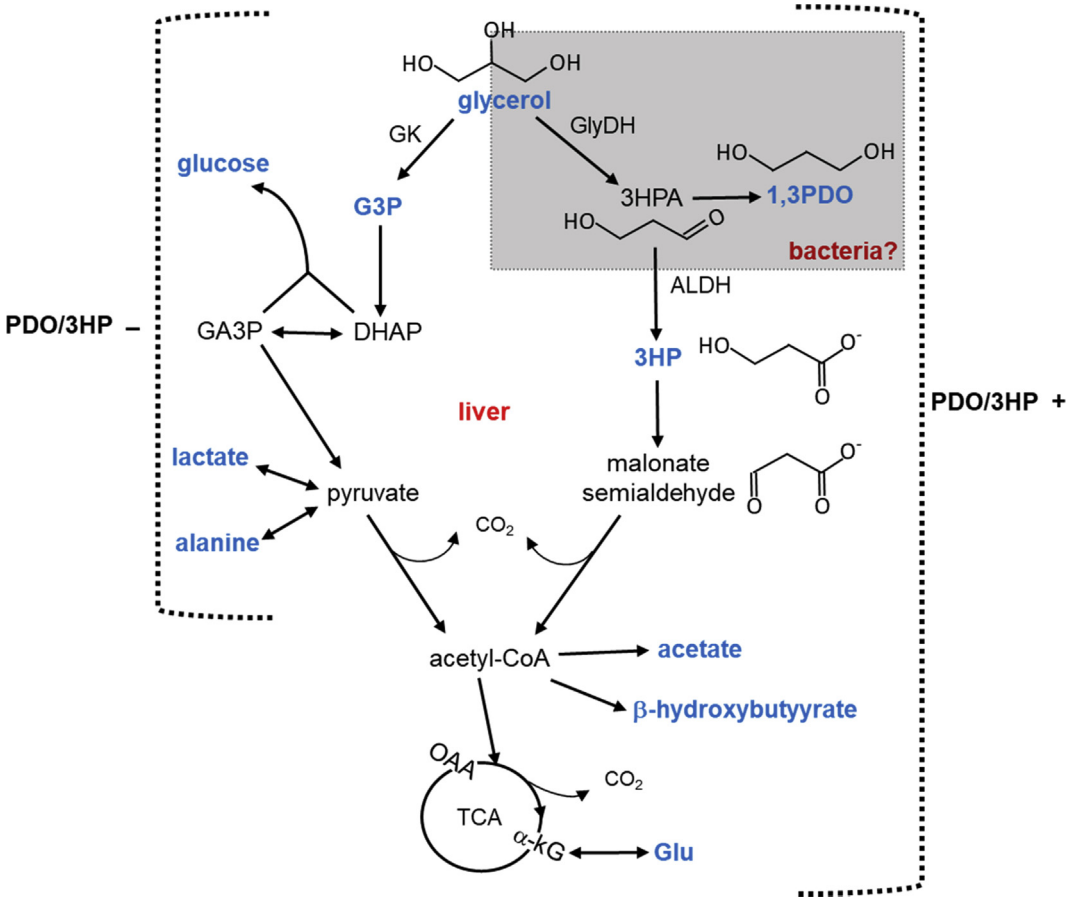


**Fig. 5. Potential alternative pathway from glycerol to acetyl-CoA in the liver with 1,3PDO and 3HP.** In the normal liver without 1,3PDO and 3HP, phosphorylated [U−$^{13}C_3$] glycerol was incorporated to gluconeogenesis or the glycolytic process. In the liver with 1,3PDO and 3HP, it is considered that 3HPA was produced from [U−$^{13}C_3$]glycerol via glycerol dehydrogenase (GlyDH) and 3HPA was metabolized to 1,3PDO possibly by bacteria. Once 3HPA was produced, it could be also metabolized to 3HP via aldehyde dehydrogenase (ALDH) in the liver. 3HP could be further metabolized to acetyl-CoA through malonate semialdehyde and consequently producing $^{13}$C-labeled acetate, β-hydroxybutyrate and glutamate. Abbreviations: DHAP, dihydroxyacetone phosphate, GA3P, glyceraldehyde 3-phosphate; G3P, glycerol 3-phosphate; Glu, glutamate; 3HPA, 3-hydroxypropionaldehyde; α-kG, α-ketoglutarate; OAA, oxaloacetate.

animals and if the metabolic changes are beneficial to the host. Though the precise role of the microbiome in production of these metabolites is uncertain, the current study demonstrated the dramatic impact of metabolites typically associated with bacteria on glycerol metabolism in the liver of the host.

## Funding

This work was supported by the National Institutes of Health [DK099289, DK058398, EB015908].

## CRediT authorship contribution statement

**Eunsook S. Jin:** Conceptualization, Methodology, Investigation, Writing – original draft, Writing – review & editing, Funding acquisition. **Min H. Lee:** Conceptualization, Methodology, Investigation. **Craig R. Malloy:** Conceptualization, Writing – review & editing, Funding acquisition.

## Declaration of competing interest

The authors declare no competing interests.

## Acknowledgements

We thank Rebecca Murphy, Xiaodong Wen and Thomas Hever for technical supports.

## References

[1] Lin EC. Glycerol utilization and its regulation in mammals. Annu Rev Biochem 1977;46:765–95. https://doi.org/10.1146/annurev.bi.46.070177.004001.
[2] Rémésy C, Demigné C. Changes in availability of glucogenic and ketogenic substrates and liver metabolism in fed or starved rats. Ann Nutr Metab 1983;27:57–70. https://doi.org/10.1159/000176624.
[3] Robinson J, Newsholme EA. The effects of dietary conditions and glycerol concentration on glycerol uptake by rat liver and kidney-cortex slices. Biochem J 1969;112:449–53. https://doi.org/10.1042/bj1120449.
[4] Davis SN, Galassetti P, Wasserman DH, Tate D. Effects of gender on neuroendocrine and metabolic counterregulatory responses to exercise in normal man. J Clin Endocrinol Metab 2000;85:224–30. https://doi.org/10.1210/jcem.85.1.6328.
[5] van der Merwe MT, Schlaphoff GP, Crowther NJ, Boyd IH, Gray IP, Joffe BI, Lönnroth PN. Lactate and glycerol release from adipose tissue in lean, obese, and diabetic women from South Africa. J Clin Endocrinol Metab 2001;86:3296–303. https://doi.org/10.1210/jcem.86.7.7670.
[6] Mallinder PR, Pritchard A, Moir A. Cloning and characterization of a gene from Bacillus stearothermophilus var. non-diastaticus encoding a glycerol dehydrogenase. Gene 1992;110(1):9–16. https://doi.org/10.1016/0378-1119(92)90438-U.
[7] Marshall JH, May JW, Sloan J. Purification and properties of glycerol: NAD+ 2-oxidoreductase (glycerol dehydrogenase) from Schizosaccharomyces pombe. Microbiology 1985;131(7):1581–8. https://doi.org/10.1099/00221287-131-7-1581.
[8] Dishisha T, Pereyra LP, Pyo SH, Britton RA, Hatti-Kaul R. Flux analysis of the Lactobacillus reuteri propanediol-utilization pathway for production of 3-hydroxypropionaldehyde, 3-hydroxypropionic acid and 1,3-propanediol from glycerol. Microb Cell Factories 2014;13:76. https://doi.org/10.1186/1475-2859-13-76.
[9] Zhu JG, Ji XJ, Huang H, Du J, Li S, Ding YY. Production of 3-hydroxypropionic acid by recombinant Klebsiella pneumoniae based on aeration and ORP controlled strategy. Kor J Chem Eng 2009;26:1679. https://doi.org/10.1007/s11814-009-0240-5.
[10] Burgé G, Saulou-Bérion C, Moussa M, Pollet B, Flourat A, Allais F, Athès V, Spinnler HE. Diversity of Lactobacillus reuteri strains in converting glycerol into 3-hydroxypropionic acid. Appl Biochem Biotechnol 2015;177(4):923–39. https://doi.org/10.1007/s12010-015-1787-8.
[11] Sobolov M, Smiley KL. Metabolism of glycerol by an acrolein-forming Lactobacillus. J Bacteriol 1960;79(2):261–6. https://doi.org/10.1128/JB.79.2.261-266.1960.
[12] Slininger PJ, Bothast RJ, Smiley KL. Production of 3-hydroxypropionaldehyde from glycerol. Appl Environ Microbiol 1983;46(1):62–7. https://doi.org/10.1128/AEM.46.1.62-67.1983.
[13] Jolly J, Hitzmann B, Ramalingam S, Ramachandran KB. Biosynthesis of 1,3-propanediol from glycerol with Lactobacillus reuteri: effect of operating variables. J Biosci Bioeng 2014;118(2):188–94. https://doi.org/10.1016/j.jbiosc.2014.01.003.
[14] Ricci MA, Russo A, Pisano I, Palmieri L, de Angelis M, Agrimi G. Improved 1,3-propanediol synthesis from glycerol by the robust Lactobacillus reuteri strain DSM 20016. J Microbiol Biotechnol 2015;25(6):893–902. https://doi.org/10.4014/jmb.1411.11078.
[15] Kumar V, Sankaranarayanan M, Durgapal M, Zhou S, Ko Y, Ashok S, Sarkar R, Park S. Simultaneous production of 3-hydroxypropionic acid and 1,3-propanediol from glycerol using resting cells of the lactate dehydrogenase-deficient recombinant Klebsiella pneumoniae overexpressing an aldehyde dehydrogenase. Bioresour Technol 2013;135:555–63. https://doi.org/10.1016/j.biortech.2012.11.018.
[16] Huang Y, Li Z, Shimizu K, Ye Q. Co-production of 3-hydroxypropionic acid and 1,3-propanediol by Klebseilla pneumoniae expressing aldH under micro-aerobic conditions. Bioresour Technol 2013;128:505–12. https://doi.org/10.1016/j.biortech.2012.10.143.
[17] Ravn K, Chloupkova M, Christensen E, Brandt NJ, Simonsen H, Kraus JP, Nielsen IM, Skovby F, Schwartz M. High incidence of propionic acidemia in Greenland is due to a prevalent mutation, 1540insCCC, in the gene for the beta-subunit of propionyl CoA carboxylase. Am J Hum Genet 2000;67(1):203–6. https://doi.org/10.1086/302971.
[18] Wilson KA, Han Y, Zhang M, Hess JP, Chapman KA, Cline GW, Tochtrop GP, Brunengraber H, Zhang GF. Inter-relations between 3-hydroxypropionate and propionate metabolism in rat liver: relevance to disorders of propionyl-CoA metabolism. Am J Physiol Endocrinol Metab 2017;313(4):E413–28. https://doi.org/10.1152/ajpendo.00105.2017.
[19] Jin ES, Lee MH, Malloy CR. Divergent effects of glutathione depletion on isocitrate dehydrogenase 1 and the pentose phosphate pathway in hamster liver. Phys Rep 2020;8:e14554. https://doi.org/10.14814/phy2.14554.
[20] Scholem RD, Brown GK. Metabolism of malonic semialdehyde in man. Biochem J 1983;216(1):81–5. https://doi.org/10.1042/bj2160081.
[21] Ando T, Rasmussen K, Nyhan WL, Hull D. 3-hydroxypropionate: significance of -oxidation of propionate in patients with propionic acidemia and methylmalonic acidemia. Proc Natl Acad Sci U S A 1972;69(10):2807–11. https://doi.org/10.1073/pnas.69.10.2807.
[22] Vollenweider S, Lacroix C. 3-hydroxypropionaldehyde: applications and perspectives of biotechnological production. Appl Microbiol Biotechnol 2004;64(1):16–27. https://doi.org/10.1007/s00253-003-1497-y.
[23] Raj SM, Rathnasingh C, Jo JE, Park S. Production of 3-hydroxypropionic acid from glycerol by a novel recombinant Escherichia coli BL21 strain. Process Biochem 2008;43:1440–6. https://doi.org/10.1016/j.procbio.2008.04.027.
[24] da Costa C, Galembeck E. The evolution of the krebs cycle: a promising subject for meaningful learning of biochemistry. Biochem Mol Biol Educ 2016;44(3):288–96. https://doi.org/10.1002/bmb.20946.
[25] Guneral F, Bachmann C. Age-related reference values for urinary organic acids in a healthy Turkish pediatric population. Clin Chem 1994;40(6):862–6. https://doi.org/10.1093/clinchem/40.6.862.
[26] Scott RS, Frame SR, Ross PE, Loveless SE, Kennedy GL. Inhalation toxicity of 1,3-propanediol in the rat. Inhal Toxicol 2005;17(9):487–93. https://doi.org/10.1080/08958370590964485.
[27] Pollitt RJ, Fowler B, Sardharwalla IB, Edwards MA, Gray RG. Increased excretion of propan-1,3-diol and 3-hydroxypropionic acid apparently caused by abnormal bacterial metabolism in the gut. Clin Chim Acta 1987;169(2–3):151–7. https://doi.org/10.1016/0009-8981(87)90314-7.
[28] Puhakainen I, Koivisto VA, Yki-Järvinen H. Lipolysis and gluconeogenesis from glycerol are increased in patients with noninsulin-dependent diabetes mellitus. J Clin Endocrinol Metab 1992;75(3):789–94. https://doi.org/10.1210/jcem.75.3.1517368.
[29] Schaefer L, Auchtung TA, Hermans KE, Whitehead D, Borhan B, Britton RA. The antimicrobial compound reuterin (3-hydroxypropionaldehyde) induces oxidative stress via interaction with thiol groups. Microbiology 2010;156:1589–99. https://doi.org/10.1099/mic.0.035642-0.
[30] Talarico TL, Dobrogosz WJ. Chemical characterization of an antimicrobial substance produced by Lactobacillus reuteri. Antimicrob Agents Chemother 1989;33(5):674–9. https://doi.org/10.1128/aac.33.5.674.